

University of Nebraska - Lincoln

DigitalCommons@University of Nebraska - Lincoln

Mechanical & Materials Engineering Faculty
Publications

Mechanical & Materials Engineering,
Department of

7-2018

Smart Bandage for Monitoring and Treatment of Chronic Wounds

Pooria Mostafalu
Harvard Medical School

Ali Tamayol
University of Nebraska-Lincoln, atamayol@uchc.edu


Rahim Rahimi
Purdue University

Manuel Ochoa
Purdue University

Akbar Khalilpour
Harvard Medical School, saba.khalilpour@unimi.it

See next page for additional authors

Follow this and additional works at: <https://digitalcommons.unl.edu/mechengfacpub>

 Part of the [Mechanics of Materials Commons](#), [Nanoscience and Nanotechnology Commons](#), [Other Engineering Science and Materials Commons](#), and the [Other Mechanical Engineering Commons](#)

Mostafalu, Pooria; Tamayol, Ali; Rahimi, Rahim; Ochoa, Manuel; Khalilpour, Akbar; Kiaee, Gita; Yazdi, Iman K.; Bagherifard, Sara; Dokmeci, Mehmet R.; Ziaie, Babak; Sonkusale, Sameer R.; and Khademhosseini, Ali, "Smart Bandage for Monitoring and Treatment of Chronic Wounds" (2018). *Mechanical & Materials Engineering Faculty Publications*. 284.
<https://digitalcommons.unl.edu/mechengfacpub/284>

This Article is brought to you for free and open access by the Mechanical & Materials Engineering, Department of at DigitalCommons@University of Nebraska - Lincoln. It has been accepted for inclusion in Mechanical & Materials Engineering Faculty Publications by an authorized administrator of DigitalCommons@University of Nebraska - Lincoln.

Authors

Pooria Mostafalu, Ali Tamayol, Rahim Rahimi, Manuel Ochoa, Akbar Khalilpour, Gita Kiaee, Iman K. Yazdi, Sara Bagherifard, Mehmet R. Dokmeci, Babak Ziaie, Sameer R. Sonkusale, and Ali Khademhosseini

Published in *Small*, 2018

doi 10.1002/sml.201703509

Copyright © 2018 WILEY-VCH Verlag GmbH & Co. KGaA, Weinheim. Used by permission.

Submitted 8 October 2017; revised: 9 April 9 2018; published 6 July 2018.

Smart Bandage for Monitoring and Treatment of Chronic Wounds

Pooria Mostafalu,^{1,2,3} Ali Tamayol,^{1,2,3,4} Rahim Rahimi,⁵

Manuel Ochoa,⁵ Akbar Khalilpour,^{1,2} Gita Kiaee,^{1,2}

Iman K. Yazdi,^{1,2} Sara Bagherifard,^{1,2}

Mehmet R. Dokmeci,^{1,2} Babak Ziaie,⁵

Sameer R. Sonkusale,⁶ and

Ali Khademhosseini^{1,2,3,7,8,9}

1 Biomaterials Innovation Research Center, Department of Medicine, Brigham and Women's Hospital, Harvard Medical School, Boston, MA 02139, USA

2 Harvard-MIT Division of Health Sciences and Technology, Massachusetts Institute of Technology, Cambridge, MA 02139, USA

3 Wyss Institute for Biologically Inspired Engineering, Harvard University, Boston, MA 02115, USA

4 Department of Mechanical and Materials Engineering, University of Nebraska–Lincoln, Lincoln, NE 68588, USA

5 Birck Nanotechnology Center, School of Electrical and Computer Engineering, Purdue University, West Lafayette, IN 47907, USA

6 Nano Lab, Department of Electrical and Computer Engineering, Tufts University, Medford, MA 02155, USA

7 Center of Nanotechnology, King Abdulaziz University, Jeddah 21569, Saudi Arabia

8 KU Convergence Science and Technology Institute, Department of Stem Cell and Regenerative Biotechnology, Konkuk University, Hwayang-dong, Kwangjin-gu, Seoul 05029, Republic of Korea

9 Department of Chemical and Biomolecular Engineering, Department of Bioengineering, Department of Radiology, California NanoSystems Institute (CNSI), University of California, Los Angeles, CA 90095, USA

Corresponding authors — A. Tamayol, *email* atamayol@unl.edu ; A. Khademhosseini, *email* khademh@ucla.edu ; S. Sonkusale, *email* sameer@ece.tufts.edu

P. Mostafalu and **A. Tamayol** contributed equally to this work and should be considered co-first authors.

Abstract

Chronic wounds are a major health concern and they affect the lives of more than 25 million people in the United States. They are susceptible to infection and are the leading cause of nontraumatic limb amputations worldwide. The wound environment is dynamic, but their healing rate can be enhanced by administration of therapies at the right time. This approach requires real-time monitoring of the wound environment with on-demand drug delivery in a closed-loop manner. In this paper, a smart and automated flexible wound dressing with temperature and pH sensors integrated onto flexible bandages that monitor wound status in real-time to address this unmet medical need is presented. Moreover, a stimuli-responsive drug releasing system comprising of a hydrogel loaded with thermo-responsive drug carriers and an electronically controlled flexible heater is also integrated into the wound dressing to release the drugs on-demand. The dressing is equipped with a microcontroller to process the data measured by the sensors and to program the drug release protocol for individualized treatment. This flexible smart wound dressing has the potential to significantly impact the treatment of chronic wounds.

Keywords: automated systems, flexible electronics, on-demand drug delivery systems, pH sensors, smart bandages, wound healing

1. Introduction

Dermal injuries can render the human body significantly vulnerable to infections.¹ Skin possesses excellent regeneration properties that allow its rapid healing upon its injury.² However, some traumatic injuries that cause significant skin damage such as burns or underlying conditions such as diabetes can overwhelm the regenerative capacity of skin.³ In such wounds, the normal healing steps of inflammation, proliferation, and maturation do not occur as expected. For example, in diabetic patients endothelial cells do not respond properly to the released cytokines and cannot support rapid angiogenesis.⁴ The low oxygen content reduces the ability of immune cells to fight environmental pathogens and thus these wound ulcers become quickly nonhealing.⁵ Studies show that over 90% of wound ulcers that were slow to heal or recurred after clinical discharge were infected with bacteria such as *Staphylococcus aureus*.⁶ The lack of proper immune response can lead to bacteremia and sepsis if the local infection is not treated effectively.⁷ As a result, chronic wounds are one of the key causes of limb amputations.

The effective protection of the body against bacterial infection requires a combinatorial method that can: (i) rapidly cover the wound and form a barrier against environmental pathogens and (ii) prevent systemic infection by its early stage detection followed by localized or systemic treatment with antibiotics. Existing dressings cover the wound bed and in some cases release therapeutic molecules passively. However, these wound dressings provide limited information about the status of the healing process

and operate in an open loop manner. Infection is a key challenge associated with chronic wounds, and patients should either be hospitalized or be continuously screened by medical professionals for signs of infection adding to treatment cost.^{7,8} Smart systems that can monitor the wound environment without the need for dressing replacement and visits to medical facilities are extremely beneficial.⁹ The emergence of flexible electronics has advanced the state-of-the-art of wearable smart biomedical devices for disease diagnosis and treatment.¹⁰ Different sensors and actuators can be integrated into a single platform capable of maintaining conformal contact with skin.^{10b-d,11} Despite these advancements, wound dressings are still primitive and cannot provide information about the wound status. The use of flexible sensors for measuring various parameters provides invaluable information helping with the selection of treatment strategy.¹² For example, one could monitor the pH of the wound environment, which is a strong indicator of bacterial infections.¹³ The pH of normal healing wounds is in the range of 5.5–6.5 during the healing phase. However, in nonhealing infected wounds, pH will be above 6.5.^{13a,14} Although blood pH can also be slightly affected by diet and diseases, the variations of wound pH in response to infection are more severe. Thus, monitoring pH could provide important data on possible infection.

Moreover, advanced medical patches can deliver therapeutics in response to the wound status in a more controlled fashion than what is possible today. Current infection therapies often require oral (systemic) and topical (e.g., on the entire wound) antibiotic administration, which need much larger dosage than would be required if administered locally (e.g., only in wound regions which need it). Such routes of antibiotic administration can also have several side effects on healthy tissues or organs. A local delivery patch, however, would overcome these drawbacks to provide more precise and controlled administration of therapeutics within the wound region to promote optimal wound healing. pH-responsive materials which function through a change in their ionization and thus the polymer state have been used for engineering self-responding drug delivery tools that can automatically release their payload.¹⁵ However, the release rate of the encapsulated antibiotics usually depends on the environment pH and might not be sufficient to remove the pathogens and create resistance. Their critical pH is also not easy-to-adjust, which limit their application for treatment of different wounds. Thus, systems that benefit from a separate stimulus for drug release might be easier to use.

As a demonstration of the potential for integrated wound monitoring and treatment using emerging flexible bioelectronics, we have engineered a platform capable of in situ detection of bacterial infection by continuously monitoring wound pH, as well as administration of antibiotics locally and on demand. The electronics feature an on-board wireless transceiver that

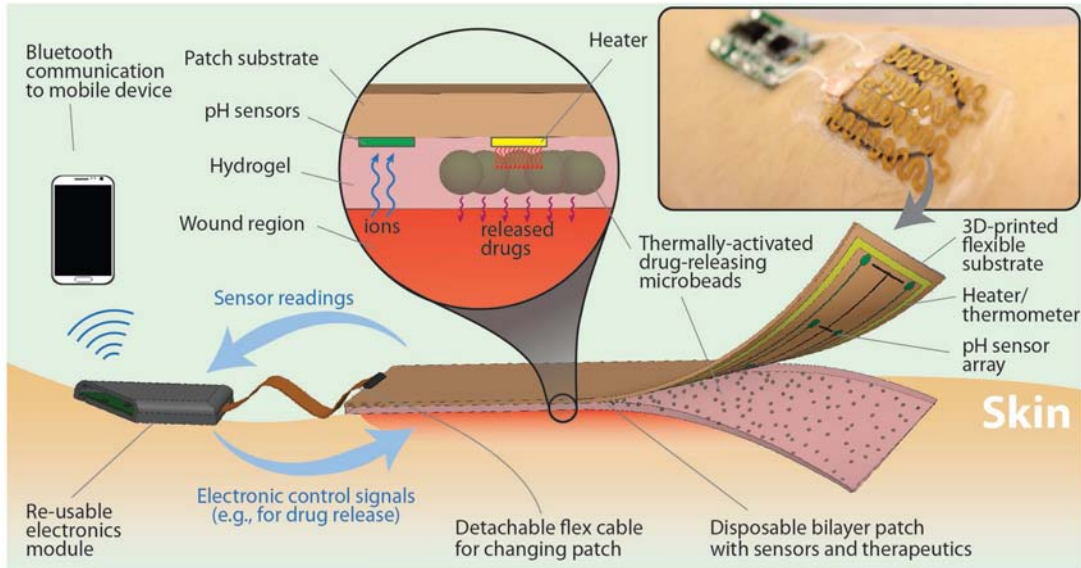


Figure 1. Schematic and conceptual view of the automated smart bandage. The bandage was comprised of an array of flexible pH sensors and a flexible heater to trigger thermo-responsive drug carriers containing antibiotics. Thermo-responsive drug carriers were embedded in a layer of alginate hydrogel which was cast around the pH sensors and on top of the flexible heater. The sensors and heater were connected to an electronic module that could record the sensors signal and power the heater if needed. The electronic module could also communicate wirelessly to computers and smartphones

transmits sensor data and can receive instructions for programmed drug release; such wireless communication capabilities serve not only to improve healing but also to maintain remote engagement among physicians, caregivers, and patients throughout the wound care process.

2. Results and Discussions

A smart bandage was engineered with multiple components including: (i) sensors (pH and temperature), (ii) microheater, (iii) thermo-responsive drug carriers embedded in a hydrogel patch, and (iv) wireless electronics to read the data from the sensors and to trigger and control the thermal actuation system if required (**Figure 1**). pH is among the key parameters for monitoring of chronic wounds. pH of a chronic wound changes from acidic to alkaline, which is typically interpreted as an indication of the bacterial infection.¹⁶ Thus, it could be used for prescreening of chronic wounds. Additionally, the temperature sensor was utilized to provide further information about the wound inflammation. Thermo-responsive drug carriers were employed for

on-demand release in response to temperature variation. For this reason, PNIPAM-based particles were fabricated and embedded within an alginate hydrogel sheet. The patch was directly cast on top of a flexible heater, which in turn was controlled using the integrated microcontroller. The entire construct was attached to a transparent medical tape to form a wearable platform that was less than 3 mm thick. The platform was engineered in a way that the sensing modules and the integrated heater were low-cost and could be disposed, while the electronics could be reused.

Potentiometric pH sensors were designed and fabricated as described in the Experimental Section.¹⁷ Carbon/polyaniline (PANI) and silver/silver chloride served as working and reference electrodes, respectively, and PANI was employed as a positive exchange membrane (**Figure 2 A–C**). The principle of operation involves protonation and deprotonation of working electrode in an acid and basic environment, where charge accumulation resulted in a voltage output that could be measured for determination of pH.

The sensor function was evaluated in terms of stability and repeatability over a wide range of pH values (from 4 to 10 and back to 4). The sensors were sequentially placed in solutions containing Na⁺ (142 mmol) and Ca²⁺ (2.5 mmol) with an ionic composition similar to human exudate with different levels of pH and the generated potential between the working and reference electrodes was measured (Figure 2D). The potential measurement of the sensor at each pH solution was recorded after reaching equilibrium state and output stability was obtained. The sensors exhibited a relatively linear response ($r^2 = 0.946$) with average sensitivity of -50 mV pH^{-1} . To evaluate stability, sensors were immersed in the highest and lowest physiological pH levels (6 and 8) and the change in the sensors potential was recorded over time. The sensor yielded a stable signal with less than 6 mV drift over a 12 h period, providing an adequate stability for wound monitoring application in which dressings are typically changed on daily basis. Currently, there is no standard test for in vitro assessment of the function of wearable sensors. Thus, to test the function of the sensor on skin, the condition was mimicked by creating agarose hydrogels (3% w/v) with different pH values. The engineered hydrogels mimic the physical properties of the wounded skin. The sensor was placed on top of them and the output signal was recorded.

A resistive microheater with resistance of 20Ω was designed and fabricated on a flexible parylene substrate, which was lightweight and FDA-approved (Figure 2F). Electrical power was transferred to the heater using electrical driver controlled by an Arduino microcontroller (LightBlue Bean, MA). The microcontroller could also communicate with external sources wirelessly, using a low-energy Bluetooth module (LightBlue Bean, MA) assembled on the electrical board. For adjusting the temperature generated by the heater and avoiding the temperature overshoot, a commercially available flexible temperature sensor (OMEGA, CT) with a linear response and

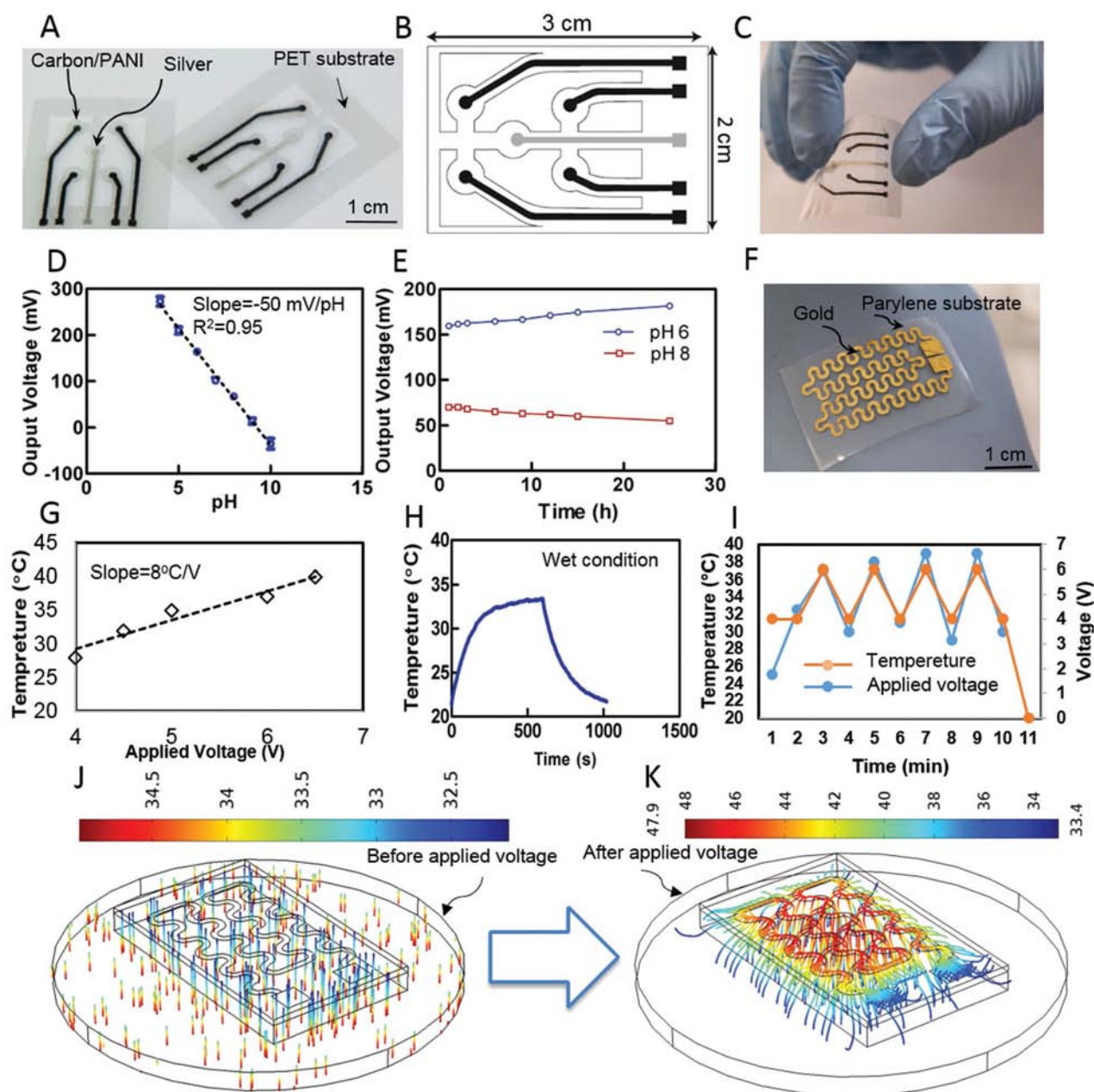


Figure 2. Sensors fabrication and characterization. **A–C)** Optical images and design of the fabricated pH sensor on PET film, carbon/PANI, and silver/silver chloride served as working electrode and reference electrode. **D)** Calibration plot of the pH sensor in range 4–10 with $r^2 = 0.95$ and sensitivity of -50 mV pH^{-1} . **E)** Transient response of the pH sensor over 24 h showing its long-term stability. **F)** Optical image of the flexible heater fabricated using gold electrodes on Parylene substrate. **G)** Calibration plot of the heater with a slope of $8 \text{ }^\circ\text{C V}^{-1}$. **H)** Transient response of the heater in a wet condition shows the response time of 5 min with applied 3 V. **I)** The temperature variation in response to cyclic application of voltage to the heater to change the platform temperature. **J,K)** Simulation for heat distribution inside the gel before and after applied electrical power, with consideration of the human skin showing that the generated heat influenced the hydrogel and did not impact on skin temperature.

sensitivity of $10 \Omega \text{ } ^\circ\text{C}^{-1}$ was assembled into the bandage next to the flexible heater. The feedback from the temperature sensor was used for adjusting the platform temperature.

The calibration graph showed that the temperature varied linearly with respect to applied electrical power (Figure 2G). Additionally, transient graph confirmed a relatively fast response of the microheater with a time response of less than 5 min (Figure 2H). To evaluate the feedback control of the platform for stabilizing the temperature, microheater in combination with the temperature sensor and electronic system was utilized. We showed the capability of the platform for dynamically switching between various temperatures. The platform was programmed to switch the temperature between 30 and 40 $^\circ\text{C}$ (Figure 2I). Distribution of the heat over the hydrogel onto skin was predicted through numerical simulation using COMSOL Multiphysics. Simulation results before and after applied electrical power confirmed precise control on temperature distribution within the hydrogel layer (Figure 2 J,K).

To be able to release antibiotics on demand, we employed stimuli-responsive drug carriers that could be triggered by applying an external stimulation. Temperature triggering mechanism was employed for delivery of antibiotics as it was safe (at temperatures lower than 42 $^\circ\text{C}$) and easy-to-apply.¹⁸ PNIPAM is a biocompatible thermo-responsive material, which can go through hydrophilic–hydrophobic transition above its critical temperature.¹⁹ PNIPAM's critical temperature is around 32 $^\circ\text{C}$, which might make the drug carriers susceptible to be self-triggered. However, PNIPAM can be grafted with other monomers or copolymerized to increase its critical temperature to $\approx 37 \text{ } ^\circ\text{C}$, reducing the possibility of undesired drug release.²⁰

PNIPAM particles were fabricated using microfluidic flow focusing approach in which the PNIPAM solution was introduced into the microchannel and was wrapped with an oil solution containing surfactant to form droplets. The size of the generated droplets could be tuned by adjusting the ratio between the flow rates of the two streams. The droplets were then crosslinked by UV irradiation. Particles with the diameter of 300 μm were fabricated, which were shrinking as being heated above 32 $^\circ\text{C}$ as shown in **Figure 3A**. This critical temperature of the PNIPAM particles makes them suitable for topical applications where the skin temperature is less than 37 $^\circ\text{C}$.

Details of the microparticle fabrication and drug release study can be found in the Experimental Section. These drug carriers were embedded into an alginate hydrogel layer (Figure 3D). A thin layer of rectangular alginate patch (2% w/v) was formed by adding solution of sodium alginate containing drug carriers into PDMS molds followed by spraying calcium chloride as a crosslinker as described elsewhere.¹⁹

To minimize the thermal contact resistance between the microheater and the hydrogel layer, the hydrogel was directly cast on top of the heater. Chronic wounds are known for their high rate of exudate generation and

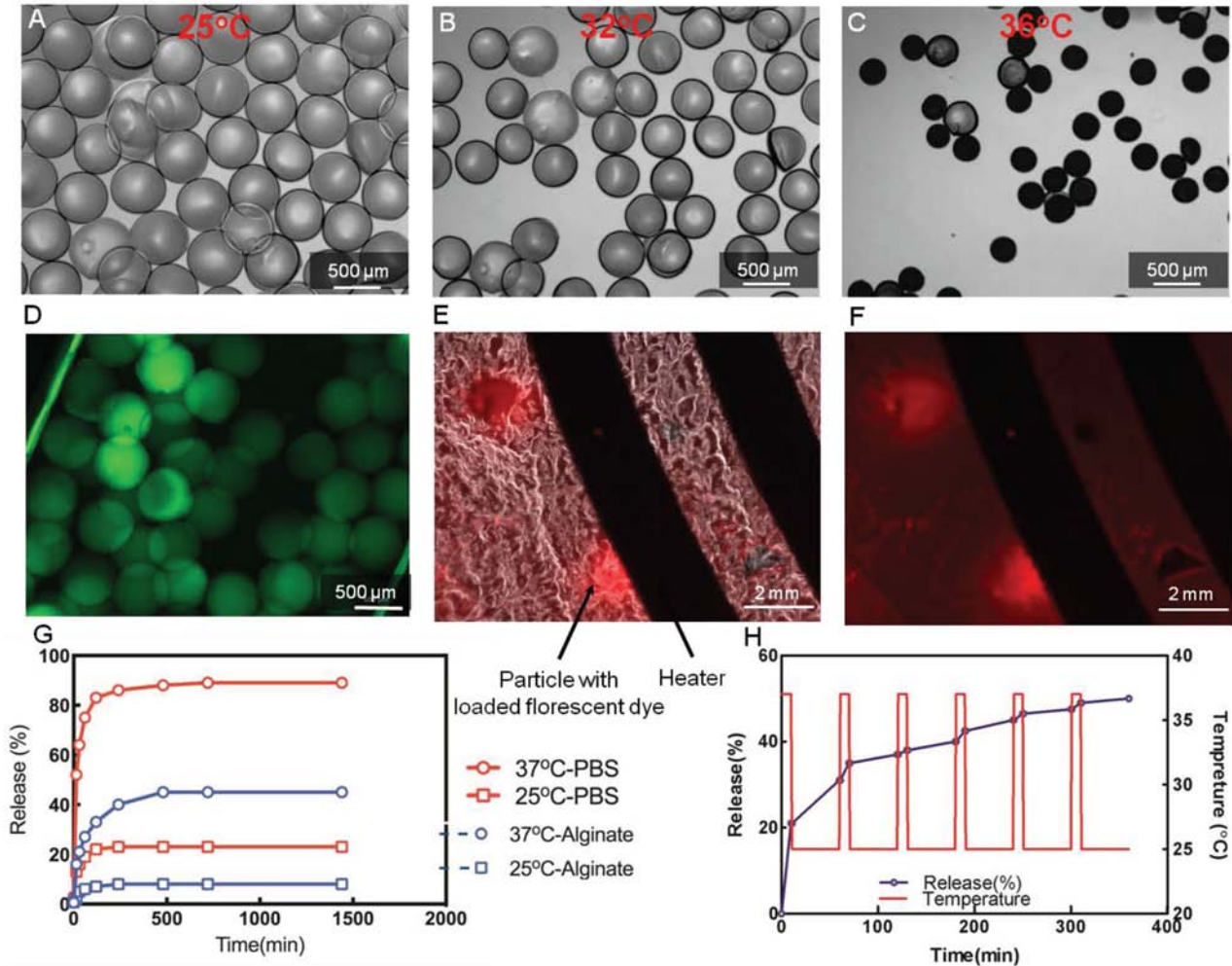


Figure 3. Drug release study. **A–C)** Optical image of the particles in a range of temperatures. **D–F)** Fluorescence images of drug carriers embedded inside the hydrogel attached to microheater, rhodamine B was used for better visualization. **G)** Release profile of cefazolin antibiotics in different temperatures and conditions. **H)** Release rate control of cefazolin by adjusting the temperature.

thus exudate management is important in the proper function of the sensors and drug delivery modules. The utilized alginate-based hydrogels are known for high water uptake and swelling ratios and have been used in engineering wet wound dressings. In addition, since the sensors are in direct contact with the skin, the swelling of the hydrogels is not expected to affect the readout. To visualize the drug release, rhodamine B was loaded into PNIPAM particles and the system was heated while being monitored under a microscope. The rhodamine B release was observed using fluorescent images (see Figure 3E,F). In order to load drugs, lyophilized PNIPAM particles were soaked in cefazolin solution (10 mg mL^{-1}) at $4 \text{ }^\circ\text{C}$. Cefazolin

is an effective antibiotics used against *S. aureus*, which is the most common bacteria in infected chronic wounds.⁶ After applying heat to the alginate patch, the cefazolin release profile was measured over time. Data suggested a quick burst release, which was followed by a controlled release of the drug; about 80% of the drug was released over 1 h. The release from drug carriers embedded within hydrogel was prolonged in comparison with those freely dispersed in phosphate buffered saline (PBS) (Figure 3G). As expected, higher temperatures led to faster release rate. To assess the possibility of releasing drugs in a dynamic fashion, heat was applied periodically (30 min on, 30 min off) and the drug release amount was determined. The results suggested that after reducing the temperature, the antibiotic release rate was significantly reduced. By reapplying heat, the drug release was restored (see Figure 3H).

A standard scratch test assay was used to evaluate the cell migration in presence of bacteria. It mimics the cell migration during healing of the infected wound and shows the efficacy of the healing. To perform this experiment, the scratch was created over a monolayer of the confluent keratinocytes, which were contaminated with *S. aureus* in advance. Three groups were used for this set of experiments: (1) cefazolin powder as a positive control, (2) alginate without antibiotic loading as a negative control, and (3) alginate containing cefazolin. The negative control showed the interaction of bacterial contamination with cell proliferation and migration observed through scratch closure. The positive control enabled us to compare the effect of antibiotics released from the patch with free antibiotics which indicated that the effectiveness of the antibiotics was not affected by thermal stimulation.

The dissolved cefazolin solution was used as a control to compare its effectiveness with the stimuli-responsive release patch made of alginate containing thermo-responsive drug carriers. Initial captured pictures showed a similar distance gap for different samples (**Figure 4**). When alginate/Ab or control samples were employed, rapid migration toward the opening area was observed. Moreover, the whole distance gap was covered with migrated cells eventually for these samples. On the other hand, the efficient migration was not seen when alginate patch without antibiotics was used.

Wound dressing should not be cytotoxic or should not negatively affect cellular growth. Although animal studies are the most suitable tool for preclinical assessment of the function of the wound care products, *in vitro* culture of human cells is also strong tool for preliminary studies. Thus, the engineered dressings were interfaced with the culture of human keratinocytes and potential toxicity of the engineered dressing was assessed. As it is shown in Figure 4E,F, the cell viability and total DNA content in presence of the antibiotic-releasing patch were similar to the control patch with viability of more than 90%.

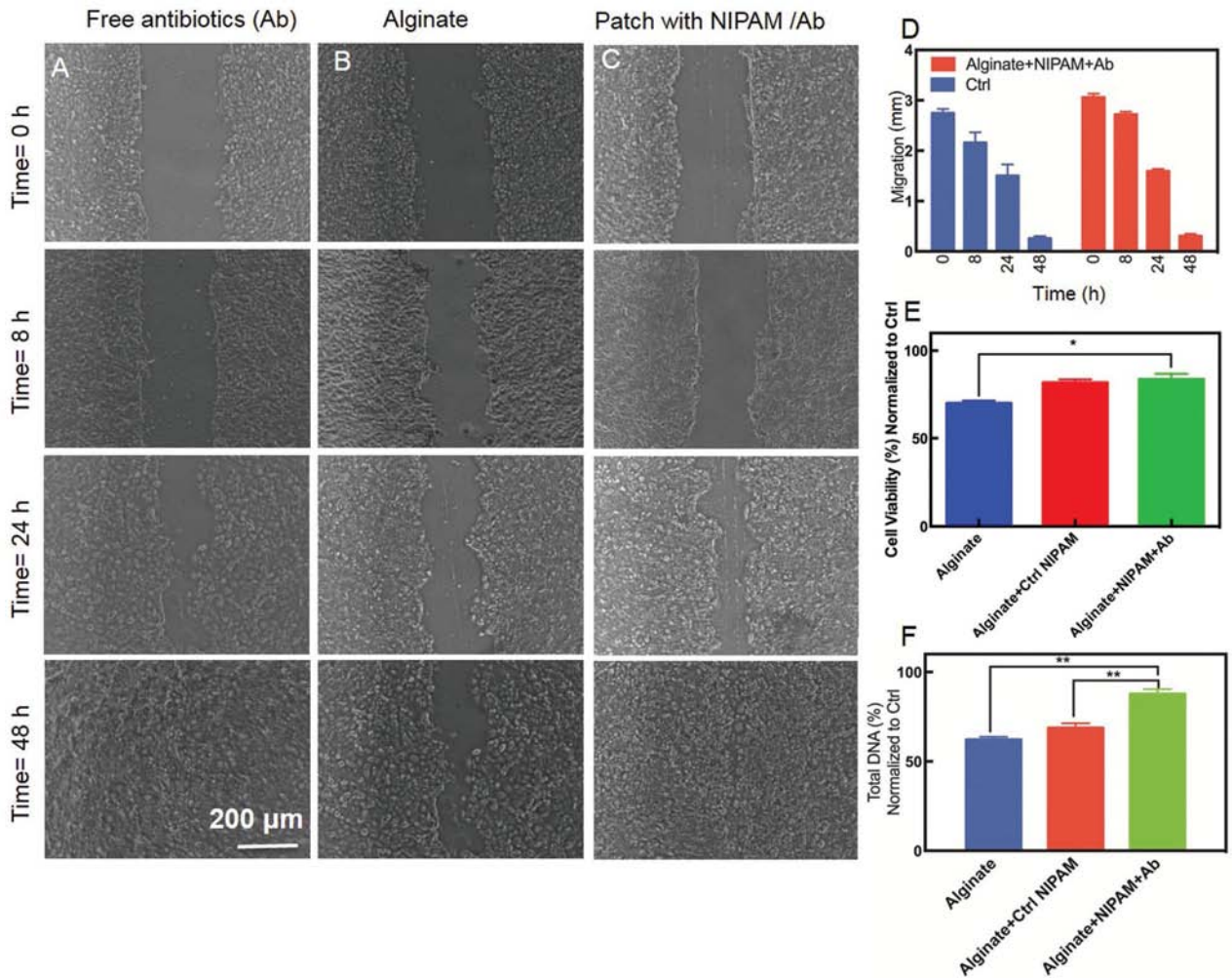


Figure 4. Scratch test assay test for evaluation of cell migration: **A)** control sample made of cefazolin solution, **B)** alginate sample without antibiotic, and **C)** antibiotic patch. **D)** Quantitative analysis of the cell migration showing the gap size on the scratch wound assay. **E,F)** Viability of keratinocyte and total DNA content as an indication of cellular proliferation in presence of the antibacterial and control samples.

To evaluate the efficacy of the thermo-responsive delivery of the antibiotics, zone of inhibition (ZOI) and number of colony-forming units (CFU) tests were performed. For the ZOI test, *S. aureus* was cultured and added on the surface of an agar plate. Then, two sets of the hydrogel patches with and without antibiotics were placed on the bacterial culture. To prepare the hydrogel patch, PNIPAM particles were loaded with cefazolin and embedded inside the alginate hydrogel. The heater was triggered to release the drug. Significant ZOI (≈ 10 mm) around the patch loaded with antibiotics was observed in comparison to the control confirming the effectiveness of the released drug in inhibiting bacterial growth (**Figure 5A,B**).

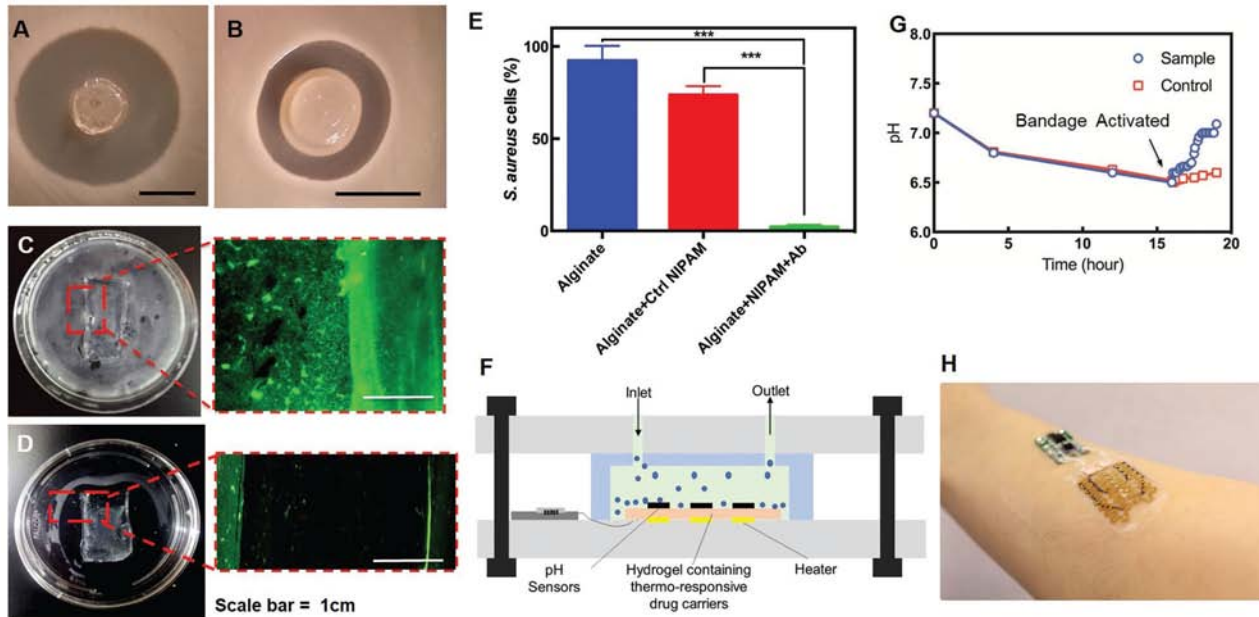


Figure 5. In vitro evaluation of the antibacterial activity of the bandage. **A,B)** Diffusion test for antibacterial releasing hydrogel and negative control (hydrogel without antibiotics). **C)** Live-dead from biofilm formation on control patch. **D)** Live-dead staining from biofilm formation on antibacterial patch; live bacteria appear as green. **E)** CFU counting test for *S. aureus* using cefazolin. **F)** Schematics of in vitro model for culturing of *S. aureus* bacteria in a bioreactor monitored with pH sensor and treated with the patch loaded with antibiotic. **G)** In vitro test showing the pH variation over time followed by the activation of the heater at pH = 6.5. **H)** The integration of the electronic component, pH sensors, microheater, and drug-loaded hydrogel. The patch was placed on the author's hand.

CFU experiment was also performed to further quantify the efficacy of the thermo-responsive antibiotic-releasing patch. While the alginate patch without antibiotics as a negative control showed $\approx 100\%$ viability ratio of the bacteria, the use of the antibiotic-loaded patch reduced their viability ratio to less than 10% (Figure 5E). Moreover, the capability of the antibiotic-eluting patch on the treatment of bacterial infection was tested on a biofilm layer of the bacteria. Bacteria were cultured on the agar plates for 4 d to create a biofilm. Then, the patch with integrated microheater was placed on the top. Live-dead assay was used after 6 h to assess the viability of bacteria at the interface of the patch. We observed that bacteria had considerable spread over the patch and the plate in the absence of the antibiotic (Figure 5C), while bacteria were killed significantly at the interface of the antibiotic eluting patch (Figure 5D).

In another experiment, a bioreactor was designed to evaluate the pH variation over the bacterial culture before and after activation of the smart patch (Figure 5F). Bacteria culture media was perfused slowly to mimic the in vivo condition. As shown in Figure 5G, when bacteria reached the lag

phase, the pH was reduced to 6.5 (the critical pH defined for the microcontroller in this experiment). At this pH, the bandage was automatically activated and cefazolin was released. pH raised up to 7.2 in the bioreactor with activated bandage whereas a stable pH was seen in the nontreated sample (deactivated bandage).

The entire platform was packaged into a flexible and wearable form that could form conformal contact with skin. A transparent medical tape was used for securing it onto skin. A typical fabricated bandage with the utilized electrical system is shown in Figure 5h.

3. Conclusions

In this work, we developed a networked closed-loop automated patch for monitoring and treatment of the chronic wounds. The closed-loop patch included sensor patch of flexible pH and temperature sensors, a hydrogel release patch with thermoresponsive drug-loaded carriers with integrated microheater, and an electronics patch. Flexible electrochemical pH sensor with linear response and sensitivity of -50 mV pH^{-1} was designed and fabricated on flexible PET substrate. According to the feedback data from pH sensor, thermo-responsive release patch was activated for the release of the antibacterial drugs. Readout from the sensor and stimulation of thermo-responsive drug were achieved remotely by taking advantage of the wireless Bluetooth low energy module in the electronics patch. The proposed bandage was characterized by *in vitro* bacterial study and subsequent antibiotic release. Additionally, scratch test assay was performed to prove the cell migration over scratch. In the proposed smart bandage, pH and temperature sensors and antibiotic drug serve as models of sensors and the drug, one could embed more sensing components, drugs, and growth factors in this platform for specific detection of particular healing marker and for treatment of different target conditions. The assessment of clinical advantage of the smart and automated (feedback controlled) dressing for facilitating the healing process of chronic wounds and its comparison to other existing technologies and wound care products requires the use of animal models that represent difficult-to-treat wounds which will be carried out in the future.

4. Experimental Section

Materials: Chemicals including sodium alginate, agarose, CaCl_2 , PNIPAM, *N,N'*-methylenebisacrylamide, and mineral oil were purchased from Sigma-Aldrich (St. Louis, MO). Irgacure 2959 (CIBA Chemicals) was used as the photoinitiator (PI). Cell culture reagents were obtained from Life Technologies, MA.

Fabrication and Characterization of pH Sensor: The pH sensors were prepared based on a previous work.¹⁷ Briefly, the pH sensor consisted of a working electrode and a solid-state Ag/AgCl reference electrode. The voltage read across the two electrodes corresponded to the pH level of the analyte solution. The fabrication process was conducted by laser-machining and screen-printing. The fabrication process starts by laser cutting a single layer of tape (3M MagicTape) to act as a stencil mask for the screen-printing process. The mask was then attached to the flexible PET substrate followed by screen-printing the carbon (MG Chemicals Graphite Conductive Coating) and silver inks (118-09, Creative Materials, Ayer, MA). After the printing process the mask was removed, revealing four working electrodes and one reference electrode. The inks were then cured in an oven set to 80 °C for 1 h.

Using the same laser machine and settings, the perimeter of electrodes was removed from the PET substrate. The openings created in the PET substrate allow the interface between the drug delivering hydrogel and the wound. Next, to prevent electrical crosstalk between the electrodes an insulating layer of poly(methyl methacrylate) (PMMA; A4) was printed onto the conductive carbon and silver traces, which defines the active area and the contact pad of the sensors. The insulating layer was cured by hot plate set to 80 °C for 10 min followed by exposing to UV light for 5 min.

The Ag/AgCl reference electrode was prepared by electrodepositing a layer of AgCl over the silver electrode. The chloridization process was performed in a solution of 1.0 M NaCl and a constant current of 1 mA for 3 min was applied across the silver electrode and a Pt electrode. The uncovered area of silver electrode changes in color with the formation of silver chloride. The resulting Ag/AgCl electrode was then rinsed with deionized water and blow dried with nitrogen.

The pH-sensitive membrane was prepared by dissolving 25 mg of polyaniline emeraldine in 10 mL dimethyl sulfoxide (DMSO), both purchased from Sigma-Aldrich, MA. For a complete dissolution, the mixture was placed in an ultrasonic bath for 2 h followed by stirring with magnetic rod for 24 h. The solution was then remained undisturbed for 24 h to allow the undissolved particles to settle. The solution was decanted and filtered through a 500 nm filter (Whatman filters) yielding a uniform dark blue solution. The working electrode was prepared by drop-casting 5 μ L volume of the pH polyaniline emeraldine base solution onto the active area of the carbon electrodes and slowly dried at 50 °C for 2 h. The polyaniline film was then doped with H⁺ ion by placing the device in a vacuum chamber with 2 mL of 1 M HCl for 5 h. The HCl fumes induced by low pressure in the vacuum chamber introduces H⁺ ions into the polyaniline emeraldine based membrane, which was then converted to polyaniline emeraldine salt. The electrodes were then rinsed with DI and dried with nitrogen.

The solid-state reference membrane was made by mixing 1:1 ratio of fine KCl powdered (Sigma-Aldrich) with UV-curable adhesive (Henkel Loctite 3105). The blend was thoroughly mixed using ultrasound, forming a uniform slurry. The slurry was then cast onto the Ag/AgCl electrode and cured under UV light for 10 min. During the UV exposure, the working electrode was protected with an aluminum foil cover. The measurements were conducted in different pH buffer solutions ranging from pH of 4 to pH of 10. The buffered solutions were purchased from Nova Analytics (Pinnacle pH Buffers). The performance of the fabricated sensors was assessed by potentiometric measurements across the pH-sensitive working electrode Ag/AgCl reference electrode with using a BASI potentiostat.

Fabrication of Microheater and Temperature Sensor: Microheater was designed and prepared based on a previous work.²¹ For fabrication of the microheater, first a glass wafer was covered by 25 μm parylene as a substrate using parylene coater (PDS2010) with 20 g of dimer. The wavy geometry of the microheater was designed in CAD software to be used as a mask. Adhesive mask was prepared with a laser cutter (Versa, VLS2.40) (power 40%, speed 20%) and attached to the substrate. A 20 nm chromium as an adhesive layer and a 200 nm gold layer were sputtered subsequently. Then, adhesive mask was peeled off and left behind a wavy pattern with 20 Ω resistance.

For the characterization of the microheater using electronic driver, constant voltage was applied using an electronic driver board.

Particle Characterization and Drug Loading: A microfluidic coflowing device was used to fabricate PNIPAM microparticles. In this system, a 10% (w/v) PNIPAM, 0.3% (w/v) *N,N*-methylene-bis-acrylamide (BIS), and 0.5% (w/v) of PI solution in water was injected through the central nozzle using a syringe pump. A solution of mineral oil containing 20% (v/v) of Span80 as surfactant was injected using another syringe pump to form a sheath around the central stream. The core flow was broken into spherical droplets and the droplet size could be tuned by changing the flow rates using two syringe pumps. Once the microdroplets have been formed, they are collected in a Petri dish and are polymerized by UV-light for 3 min in the temperature around 4 $^{\circ}\text{C}$ and the UV intensity of 850 mW and the distance between the tip of the fiber optic and the Petri dish is set to 6 cm. Subsequently, the microhydrogels were washed with ethanol and distilled water several times to remove the environmental oil and then were verified under microscope visually, after that the particles were freeze-dried and stored in 4 $^{\circ}\text{C}$ for future experiments.

The freeze-dried microcarriers were immersed in distilled water with drug (concentration) and they swell promptly to their original size while absorbing the drug. When temperature reached above lower critical solution temperature (LCST) phase transition occurred and the particles change

from hydrophilic polymer to a hydrophobic polymer, this alteration led to an ejection of water. This drying and swelling behavior was a reversible process that did not cause morphological damage.

Drug Release with Integrated Heaters: Alginate hydrogel with embedded drug microcarriers was attached on the surface of the microheater while 200 μL PBS was added into the plate and electrical voltage was applied to generate heat. The drug released into the solution was evaluated using plate reader.

Bacterial Study: A single colony of *S. aureus* was inoculated into 10 mL liquid broth (LB) culture medium overnight. For preparation of the fresh bacteria solution, 100 μL of this sample were added to a 10 mL LB and incubated at 36 °C, 200 rpm overnight. After being incubated and reaching OD600 of ≈ 0.4 , 1 mL of the fresh bacteria was spread on an LB agar plate, the strain enters the exponential period of growth and the culture broth was diluted. Bacteria with the concentration of $\approx 1 \times 10^5$ cells mL^{-1} were cultured for ZOI and CFU counting experiments. To investigate the application of device on bacteria, the device was placed on the surface of cultured bacteria, and different electrical voltages were applied to the conductive pattern to generate heat. A blank control sample without antibiotics was prepared for comparison. All the plates were incubated at 37 °C for an appropriate time. Finally, the plates were taken out of the incubator and the ZOI and number of remaining CFUs were calculated.

Scratch Wound Healing Assay and Cell Studies: Adult Normal Human Epidermal Keratinocytes purchased from ATCC were cultured in a DMEM-based medium containing 10% FBS and 1% penicillin/ streptomycin. For cytotoxicity assessment, circular samples (1 cm in diameter) were prepared and placed at the bottom of 24-well polystyrene plates. Then, cells were resuspended in culture media at the concentration of 1×10^7 cells mL^{-1} and 5000 cells were seeded on the samples. The samples were incubated for 1 h to allow the cells to attach and then 300 μL of culture medium was added to each well. Cellular metabolic activity was measured using PrestoBlue assay on days 1, 3, and 7 as per manufacturer's protocol. The fluorescent intensity of the assay was measured using a BioTek UV/vis Synergy 2 microplate reader.

Keratinocytes (1×10^5) were seeded and cultured in a six-well plate and kept overnight to make a confluent monolayer overnight. The 1 mm wide gap scratch was then created onto the monolayer with a 200 μL pipette tip, and floating cells were removed by twice washing with PBS. After the line scratches, 2 mL of DMEM was added for each group. To detect the efficacy of treatments on cell migration, samples were continually imaged for 0, 8, 24, and 48 h. Images of the monolayer were taken by a microscope and cell

migration activity was evaluated as the migration distance from the edges of the scratch toward the center of it using Image J software (NIH, Bethesda, MD, USA). For each well, ten images were taken and selected randomly. Experiments were done independently in triplicate.

Acknowledgments — This work was supported by the National Science Foundation (EFRI-1240443), the Office of Naval Research Young Investigator award, ONR PECASE Award, and the National Institutes of Health (AR066193, AR066193, EB022403, AR057837, HL137193, EB021857, and EB024403). I.K.Y. acknowledges financial support from the NIH through the Organ Design and Engineering Training program (T32 EB16652).

Disclosures — The authors declare no conflict of interest.

References

- [1] Y. Bayram, M. Parlak, C. Aypak, I. Bayram, *Int. J. Med. Sci.* **2013**, *10*, 19.
- [2] A. J. Singer, R. A. Clark, *N. Engl. J. Med.* **1999**, *341*, 738.
- [3] T. Bjarnsholt, K. Kirketerp-Møller, P. Ø. Jensen, K. G. Madsen, R. Phipps, K. Kroghfelt, N. Høiby, M. Givskov, *Wound Repair Regener.* **2008**, *16*, 2.
- [4] a) H. A. Hadi, J. Al Suwaidi, *Vasc. Health Risk Manage.* **2007**, *3*, 853; b) M. G. Tonnesen, X. Feng, R. A. Clark, *J. Invest. Dermatol. Symp. Proc.* **2000**, *5*, 40.
- [5] G. S. Schultz, R. G. Sibbald, V. Falanga, E. A. Ayello, C. Dowsett, K. Harding, M. Romanelli, M. C. Stacey, L. Teot, W. Vanscheidt, *Wound Repair Regener.* **2003**, *11*, S1.
- [6] J. S. Boateng, K. H. Matthews, H. N. Stevens, G. M. Eccleston, *J. Pharm. Sci.* **2008**, *97*, 2892.
- [7] G. A. James, E. Swogger, R. Wolcott, P. Secor, J. Sestrich, J. W. Costerton, P. S. Stewart, *Wound Repair Regener.* **2008**, *16*, 37.
- [8] R. Edwards, K. G. Harding, *Curr. Opin. Infect. Dis.* **2004**, *17*, 91.
- [9] S. Saghzadeh, C. Rinoldi, M. Schot, S. S. Kashaf, F. Sharifi, E. Jalilian, K. Nuutila, G. Giatsidis, P. Mostafalu, H. Derakhshandeh, K. Yue, W. S. A. Memic, A. Tamayol, A. khademhosseini, *Adv. Drug Delivery Rev.* **2018**, *127*, 138.
- [10] a) P. Mostafalu, S. Sonkusale, *Biosens. Bioelectron.* **2014**, *54*, 292; b) S. Bauer, *Nat. Mater.* **2013**, *12*, 871; c) D.-H. Kim, N. Lu, R. Ma, Y.-S. Kim, R.-H. Kim, S. Wang, J. Wu, S. M. Won, H. Tao, A. Islam, *Science* **2011**, *333*, 838; d) J. A. Rogers, T. Someya, Y. Huang, *Science* **2010**, *327*, 1603.
- [11] a) A. H. Najafabadi, A. Tamayol, N. Annabi, M. Ochoa, P. Mostafalu, M. Akbari, M. Nikkhah, R. Rahimi, M. R. Dokmeci, S. Sonkusale, *Adv. Mater.* **2014**, *26*, 5823; b) W. H. Yeo, Y. S. Kim, J. Lee, A. Ameen, L. Shi, M. Li, S. Wang, R. Ma, S. H. Jin, Z. Kang, *Adv. Mater.* **2013**, *25*, 2773.

- [12] a) N. Lu, C. Lu, S. Yang, J. Rogers, *Adv. Funct. Mater.* **2012**, 22, 4044; b) L. Gao, Y. Zhang, V. Malyarchuk, L. Jia, K.-I. Jang, R. C. Webb, H. Fu, Y. Shi, G. Zhou, L. Shi, *Nat. Commun.* **2014**, 5, 4938.
- [13] a) L. A. Schneider, A. Korber, S. Grabbe, J. Dissemmond, *Arch. Dermatol. Res.* **2007**, 298, 413; b) M. C. Varghese, A. K. Balin, D. M. Carter, D. Caldwell, *Arch. Dermatol.* **1986**, 122, 52; c) R. F. Diegelmann, M. C. Evans, *Front. Biosci.* **2004**, 9, 283; d) A. Tamayol, M. Akbari, Y. Zilberman, M. Comotto, E. Lesha, L. Serex, S. Bagherifard, Y. Chen, G. Fu, S. K. Ameri, W. Ruan, E. L. Miller, M. R. Dokmeci, S. Sonkusale, A. Khademhosseini, *Adv. Healthcare Mater.* **2016**, 5, 711.
- [14] R. Rahimi, M. Ochoa, A. Tamayol, S. Khalili, A. Khademhosseini, B. Ziaie, *ACS Appl. Mater. Interfaces* **2017**, 9, 9015.
- [15] N. Ninan, A. Forget, V. P. Shastri, N. H. Voelcker, A. Blencowe, *ACS Appl. Mater. Interfaces* **2016**, 8, 28511.
- [16] D. M. Ansell, J. E. Kloepper, H. A. Thomason, R. Paus, M. J. Hardman, *J. Invest. Dermatol.* **2011**, 131, 518.
- [17] R. Rahimi, M. Ochoa, T. Parupudi, X. Zhao, I. K. Yazdi, M. R. Dokmeci, A. Tamayol, A. Khademhosseini, B. Ziaie, *Sens. Actuators, B* **2016**, 229, 609.
- [18] A. Tamayol, A. H. Najafabadi, P. Mostafalu, A. K. Yetisen, M. Comotto, M. Aldhahri, M. S. Abdel-wahab, Z. I. Najafabadi, S. Latifi, M. Akbari, N. Annabi, S. H. Yun, A. Memic, M. R. Dokmeci, A. Khademhosseini, *Sci. Rep.* **2017**, 7, 9220.
- [19] S. Bagherifard, A. Tamayol, P. Mostafalu, M. Akbari, M. Comotto, N. Annabi, M. Ghaderi, S. Sonkusale, M. R. Dokmeci, A. Khademhosseini, *Adv. Healthcare Mater.* **2016**, 5, 175.
- [20] P. Mostafalu, G. Kiaee, G. Giatsidis, A. Khalilpour, M. Nabavinia, M. R. Dokmeci, S. Sonkusale, D. P. Orgill, A. Tamayol, A. Khademhosseini, *Adv. Funct. Mater.* **2017**, 27, 1702399.
- [21] P. Mostafalu, S. Amugothu, A. Tamayol, S. Bagherifard, M. Akbari, M. R. Dokmeci, A. Khademhosseini, S. Sonkusale, presented at IEEE Biomedical Circuits and Systems Conf. (BioCAS), Atlanta, GA, USA, October **2015**.